PREDICTION OF THE DISTRIBUTION AREA AND ENVIRONMENTAL VARIABLES OF *POPULUS EUPHRATICA* AND *POPULUS PRUINOSA* IN CHINA BASED ON THE OPTIMIZED MAXENT MODEL

WANG, Z. J.[1,2#] – GAI, Z. S.[1,2#] – YANG, T. G.[3] – ZHAI, J. T.[1,2] –WU, Z. H.[2,4] – GUO, X. F.[1,2] – CHEN, X. X.[1,2] – SUN, J. H.[1,2] – JIAO, P. P.[1,2*] – LI, Z, J.[1,2*]

[1]*Xinjiang Production & Construction Corps Key Laboratory of Protection and Utilization of Biological Resources in Tarim Basin/Research Center of Populus Euphratica, Alar, 843300 Xinjiang, China*

[2]*College of Life Science and Technology, Tarim University, Alar, 843300 Xinjiang, China*

[3]*Hubei Provincial Key Laboratory for Protection and Application of Special Plant Germplasm in Wuling Area of China, College of Life Sciences, South Central Minzu University, Wuhan, 430074 Hubei, China*

[4]*College of Life Sciences, Zhejiang Normal University, Jinhua, 321004 Zhejiang, China*

[#]*These authors contributed equally to this work*

**Corresponding authors*
e-mail: jiaopeipei2000@126.com, lizhijun0202@126.com; phone: + 86-997-468-1202

(Received 11th Feb 2023; accepted 27th Apr 2023)

Abstract. *Populus euphratica* (*Pe*) and *Populus pruinosa* (*Pp*) are important dominant species for maintaining ecological balance in desert and arid areas. Understanding the distribution of potentially suitable areas of *Pe* and *Pp* in arid areas is of great significance for the protection and restoration of natural *Pe* and *Pp* forests. The optimized MaxEnt was used to reconstruct and predict the potential suitable areas of *Pe* and *Pp* in China, and calculate the migration of distribution center points. The results showed that (1) the geographical distribution of *Pe* was mainly affected by coldest month minimum temperature (Bio6), mean Temperature of Warmest Quarter (Bio10). The geographical distribution of *Pp* was mainly affected by coldest month minimum temperature (Bio6), temperature Annual Range (Bio7); (2) under the current climatic scenarios, the potential suitable areas of *Pe* and *Pp* in China are 141.16 × 10^4 km^2 and 172.25 × 10^4 km^2;(3) The niche overlap D and I values of *Pe* and *Pp* were 0.533 and 0.775 respectively; (4) under the future climate scenario, the potential high-fitness area of *Pe* and *Pp* would shift to higher latitudes. Our research provides a scientific basis for the long-term protection and management of these rare natural resources.
Keywords: *potentially suitable area, climate change, environmental protection*

Introduction

Current human activities and the use of fossil energy have accelerated global warming (Bandh et al., 2021; Hou et al., 2021). Climate warming directly leads to the emergence of extreme climates such as drought, flood, high temperature, and low temperature (Liu et al., 2021). Temperature and precipitation are the two most critical climate variables affecting species distribution (Cong et al., 2020). Many studies have shown that with the changes in temperature and precipitation, the areas suitable for vegetation growth will change. Temperature rise may force vegetation to migrate to high-latitude and high-altitude areas (Guan et al., 2022; Guo et al., 2017; Li et al., 2022a; Li et al., 2022b).

http://www.aloki.hu ● ISSN 1589 1623 (Print) ● ISSN 1785 0037 (Online)
DOI: http://dx.doi.org/10.15666/aeer/2104_32233241

Species distribution models (SDMs) can evaluate the relationship between the species records for specific sites and the environmental and spatial characteristics of these sites. Therefore, SDMs are widely used in biogeography, conservation biology, and ecological research (Guisan et al., 2004, 2000; Peterson, 2006). Among them, MaxEnt is one of the most commonly used and accurate modeling methods (Phillips et al., 2009). MaxEnt is superior to other modeling methods in that it uses only existing data to achieve high prediction performance (Gomes et al., 2018). In addition, MaxEnt uses continuous and classified data to avoid errors (Elith et al., 2011). It also combines the interaction between different variables and shows the best prediction ability when using different sample sizes (Pennino et al., 2018).

Populus euphratica (*Pe*) and *Populus pruinosa* (*Pp*) are deciduous trees belonging to the genus Populus of Salicaceae. The natural distribution areas of *Pe* range from western China and the Middle East to North Africa and southwestern Europe (Wang et al., 2014, 2011). *Pp* is mainly restricted to Xinjiang province in China and the adjacent countries and regions (Wang et al., 2011). The distribution range of *Pp* is much smaller than that of *Pe*, and the two are often mixed in southern of Xinjiang, China. Research on predicting the potential distribution area of *Pe* by the optimized MaxEnt model has been reported, for example, Li et al. (2020) and Zhang et al. (2020) found that the dominant variables affecting the distribution of *Pe* were the precipitation in wettest month and annual average temperature. The high-fitness area of *Pe* is mainly distributed in the central and western regions of Inner Mongolia and most regions of Xinjiang (Li et al., 2020; Zhang et al., 2020). Chen et al. (2021a) believed that the dominant variables affecting the distribution of *Pe* are average temperature and altitude in the driest season, and the high fitness area of *Pe* is distributed in the Aksu River basin (Chen et al., 2021a). Zeng et al. (2018) estimated the distribution of *Pe* under the paleoclimate and current climate, and the results showed that *Pe* had good suitability in Xinjiang, northern Gansu, and western Inner Mongolia (Zeng et al., 2018).

However, there is no research report on identifying potential *Pp* suitable areas based on the optimized MaxEnt model, and the prediction of suitable areas and comparison of main environmental variables of *Pe* and *Pp* under the influence of current climate and geographical factors. In this paper, the optimized MaxEnt model and ArcGIS software were used to predict the suitable areas of *Pe* and *Pp* in China and the dominant environmental variables that affect their distribution, to explore the contribution of different environmental variables to the distribution of *Pe* and *Pp* in the suitable areas, to analyze the current potential suitable habitat, and to predict the changes of the suitable areas under the next four climate scenarios. This study provides a scientific basis for protecting *Pe* and *Pp* forest resources and restoring degraded ecosystems in the future.

Materials and methods

Sample distribution of Pe and Pp

Combined with the field sampling survey (Firstly, we obtained population information through literature review and collaboration with various forestry departments in China. In 2021, we conducted a field survey, covering a total distance of over 40000 km. The survey locations included Xinjiang, Qinghai, Inner Mongolia, Ningxia, and Gansu in China.), the distribution areas of *Pe* and *Pp* in China were obtained through GPS positioning (Gai et al., 2021; Chen et al.,2021). The foreign data of *Pp* and *Pe* are obtained from GBIF the GBIF database of the Global Biodiversity

http://www.aloki.hu ● ISSN 1589 1623 (Print) ● ISSN 1785 0037 (Online)
DOI: http://dx.doi.org/10.15666/aeer/2104_32233241

Information network (https://www.gbif.org/, December 13, 2022). Finally, a total of 576 distribution points of *Pe* and 608 distribution points of *Pp* were obtained (Among them, 77 *Pe* data information came from GBIF, and 499 data information came from field survey in 2022. 5 *Pp* data information came from GBIF, and 604 data information came from field survey in 2022). Only one occurrence record was kept for each 2.5 × 2.5 km raster interval to prevent overfitting of the model using the ENMtools software for the species occurrence records (Warren et al., 2021; Zhou et al., 2022). Once filtering was complete,187 distribution points of *Pe* and 107 distribution points of *Pp* data were reserved for model construction (*Fig. 1*).

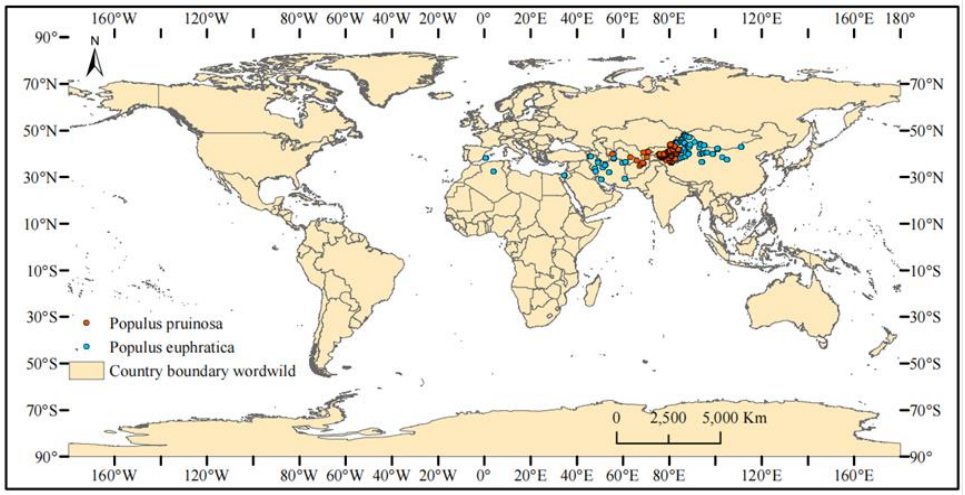

Figure 1. *Global distribution map of Populus euphratica and Populus pruinosa*

Environmental variables

There were 19 environmental variables (1971-2000) and 1 altitude variable include in this paper (*Table 1*). The data of temperature and precipitation climate variable data were from the World Climate Database v2.1 (WorldClim; https://www.worldclim.org/, December 13, 2022). And the environmental variables were converted into the same data format (ASCII) so that they could be loaded directly with MaxEnt software. The future data included two typical CO_2 representative shared socioeconomic pathways SSP1-2.6 and SSP5-5.8. Then, the distribution of *Pe* and *Pp* under four future scenarios under shared socioeconomic pathways (SSPS) was systematically analyzed: 2050s, SSP1-2.6, 2050s, SSP5-85, 2090s, SSP12.6, 2090s, SSP5-8.5.

Environmental variable filtering

The most important factor in species distribution modeling was the selection of variables (Fourcade et al., 2018). Removing redundant variables can further enhance the analysis ability of the model and reduce the multicollinearity between variables (Yi et al., 2016). To evaluate the accuracy of modeling, it was necessary to carry out the correlation coefficient test based on the combination of environmental variables (Dai et al., 2022). First, ENMtools (environmental niche modeling tools) software was used to conduct correlation coefficient analysis (Yan et al., 2015), selected the environmental variables with correlation coefficient with absolute values greater than or equal to 0.8 (*Fig. A1*) (Warren et al., 2021; Anand et al., 2021; Fourcade et al., 2014).

http://www.aloki.hu ● ISSN 1589 1623 (Print) ● ISSN 1785 0037 (Online)
DOI: http://dx.doi.org/10.15666/aeer/2104_32233241

Table 1. *Environmental variables used in MaxEnt model*

Environment variable	Description	Unit
Bio1	Annual mean temperature	℃
Bio2	Mean diurnal range	℃
Bio3	Isothermality (Bio2/Bio7) (*100)	-
Bio4	Temperature Seasonality (*100)	-
Bio5	Max temperature of warmest month	℃
Bio6	Min temperature of coldest month	℃
Bio7	Temperature annual range (Bio5-Bio6)	℃
Bio8	Mean temperature of wettest quarter	℃
Bio9	Mean temperature of driest quarter	℃
Bio10	Mean temperature of warmest quarter	℃
Bio11	Mean temperature of coldest quarter	℃
Bio12	Annual precipitation	mm
Bio13	Precipitation of wettest month	mm
Bio14	Precipitation of driest month	mm
Bio15	Precipitation seasonality (coefficient of variation)	-
Bio16	Precipitation of wettest quarter	mm
Bio17	Precipitation of driest quarter	mm
Bio18	Precipitation of warmest quarter	mm
Bio19	Precipitation of coldest quarter	mm
Elve	Altitude	m

Optimization of model parameters

We used the Kuenm package to optimize the regularization multiplier (RM) and feature combinations (FCs) parameters in the R software (Cobos et al., 2019). These two parameters were essential for building the species distribution model using the software MaxEnt (https://biodiversityinformatics.amnh.org/open_source/maxent/). In all 232 candidate models, with parameters reflecting all combinations of 8 (RMs) settings (from 0.5 to 4, the interval is 0.5) and 29 (FCs) were evaluated. Model selection was based on statistical significance (partial ROC), and complexity (AICc values). First, candidate models were screened to keep those that were statistically significant; finally, the models with lowest delta_AICc values were select among the significant candidate models (Zhu et al., 2014). *Pe*'s FCs and RM were set to TH and 1. *Pp*'s FCs and RM were set to LQP and 0.5.

Model evaluation and potential suitable area delineation accuracy

The longitude and latitude information of *Pe* and *Pp* and the filtered environmental variable data are imported into MaxEnt v3.4.1 software for modeling operations. The FC and RM were set up according to the optimal model, 75% of the sample data were randomly selected in training, while 25% of the sample data were used for testing (Yi et al., 2016; Moreno et al., 2011). In the MaxEnt model, the background points to 10,000, the maximum number of iterations was set to 500, the output format to Cloglog, and cross-validated by running 10 replicates.

http://www.aloki.hu ● ISSN 1589 1623 (Print) ● ISSN 1785 0037 (Online)
DOI: http://dx.doi.org/10.15666/aeer/2104_32233241

The jackknife test was chosen to test and create response curves (Wang et al., 2017). The ASCII format file loaded by ArcGIS was resampled, and the potentially suitable areas were classified by "Jenks' natural breaks" (Hebbar et al., 2022). According to IPCC's explanation of the probability (P) of species' presence: $P \leq 0.1$ is the unsuitable area; $0.1 < P \leq 0.5$ is the poorly suitable area; $0.5 < P$ is a high fitness area (Hanley, 1982).

The receiver operating characteristic (ROC) curve (AUC) was used to evaluate model performance (Manzoor et al., 2020). AUC values close to 1 represent perfect predictions (Wang et al., 2021). The model performance was divided into five grades according to the AUC value: poor (0-0.5), usable (0.5-0.8) and excellent (0.8-1.0) (Liu et al., 2013). The smallest difference between the training and test AUC data (AUCDiff) was also observed; a lower difference indicates less overfitting in the model (Mao et al., 2017).

Comparison of geographical distribution and niche

Use ENMTools calculated the niche overlap and geographic distribution coincidence degree of *Pp* and *Pe*, the threshold value of geographical distribution was 0.5. Schoener's D (D) and Hellinger's based I (I) values were used to indicate the niche overlap. The D and I values are between 0 and 1. The larger the values, the more niche overlap (Dan et al., 2010).

Distribution and center transfer of suitable growing areas of Pe and Pp in the future climate data

After modeling the currently relevant areas of *Pe* and *Pp*, the size of the potential distribution areas was calculated. Future climate data were used to model and predict, and calculate the suitable area for growth in the future. To further understand the future migration path and direction of *Pe* and *Pp*, the centroid of *Pe* and *Pp* from the current distribution to the future distribution was calculated using the Python-based SDM toolbox (Brown et al., 2017; Manzoor et al., 2020). This analysis concentrates the distribution of species to an independent central point and creates a vector file that describes the size and direction of species over time (Wang et al., 2021). We observed the change in distribution by calculating the change in centroid in different periods in the future.

Results

Accuracy detection of the prediction results of the MaxEnt model by ROC curve

The result showed that delat_AICc was lowest when *Pe*'s FCs are TH and RM is 1, *Pp*'s FCs were LQP and RM was 0.5 (*Fig. 2*). Under the optimal parameter settings, the mean AUC value based on the MaxEnt model for the current potential habitat area of *Pe* was 0.979, *Pp* was 0.989, indicating excellent model prediction accuracy (*Fig. 3*). In addition, the average of AUCDiff of *Pe* was 0.0079, *Pp* was 0.004, indicating less overfitting in the model.

Dominant environmental variables

The coldest month minimum temperature (Bio6), the mean Temperature of Warmest Quarter (Bio10), the coldest quarterly average temperature (Bio11) and the warmest quarterly precipitation (Bio18) were made great contributions to the establishment of the

http://www.aloki.hu ● ISSN 1589 1623 (Print) ● ISSN 1785 0037 (Online)
DOI: http://dx.doi.org/10.15666/aeer/2104_32233241

model for *Pe* (*Fig. 4A*). The coldest month minimum temperature (Bio6), the temperature Annual Range (Bio7), and the coldest quarterly average temperature (Bio11) were made great contributions to the establishment of the model for *Pp* (*Fig. 4B*).

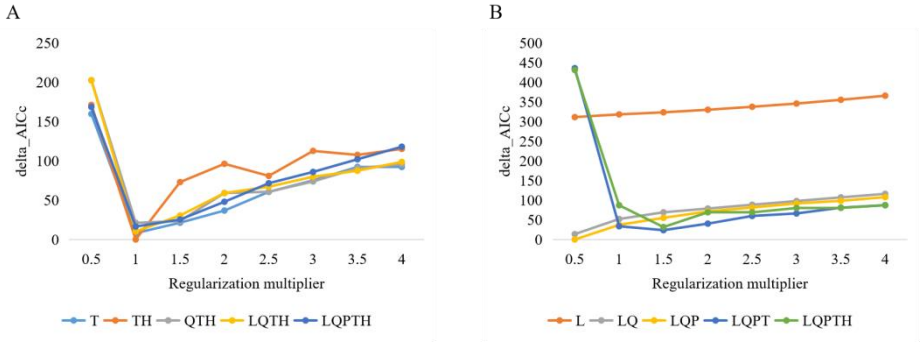

Figure 2. *Optimal parameter results of Populus euphratica (A) and Populus pruinosa (B) for the MaxEnt model*

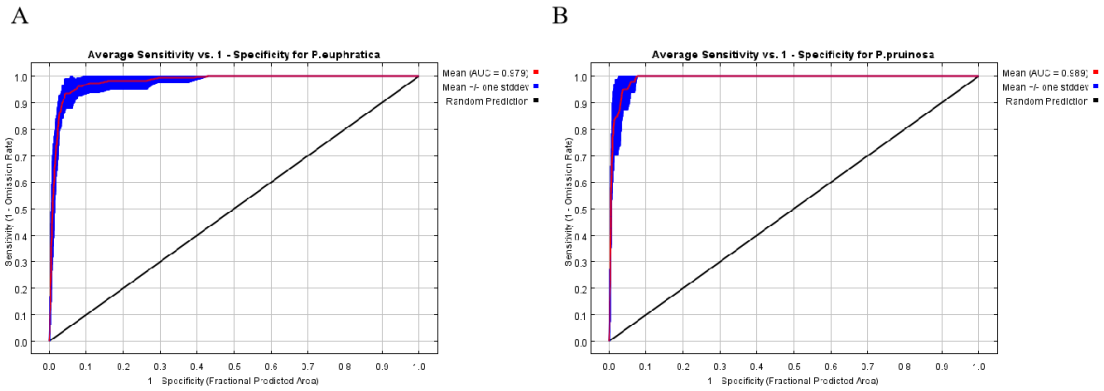

Figure 3. *ROC curve for Populus euphratica (A) and Populus pruinosa (B) using the MaxEnt*

The response curve of the model represents the influence trend of each environmental variable on the prediction of the model. Combined with the contribution rate and the test results of the Jackknife test, the response curve of five environmental variables on the fitness of *Pe* (*Fig. 5*) and the response curve of five environmental variables on the fitness of *Pp* (*Fig. 6*) were obtained. The relationship between the distribution probability of *Pe* and *Pp* and environmental variables could be judged according to the response curve of environmental variables. It is generally believed that when the distribution probability of *Pe* and *Pp* is more than 0.5, the value of their corresponding environmental variables is suitable for the growth of *Pe* and *Pp*. The dominant environmental variables in *Pe* suitable areas were as follows: the lowest temperature in the coldest month (Bio6) was -19 ~ -10℃, the mean Temperature of Warmest Quarter (Bio10) was 22-26℃ the average temperature in the coldest quarter (Bio11) was -10 ~ -2℃, and the precipitation in the warmest quarter (Bio18) was 14 ~ 64 mm. The dominant environmental variables in the suitable growth area of *Pp* were as follows: the lowest temperature in the coldest month (Bio6) was -16 ~ -8℃, the temperature Annual Range (Bio7) was 42 ~ 52℃, the average temperature in the coldest quarter (Bio11) was -7 ~ -1℃.

http://www.aloki.hu ● ISSN 1589 1623 (Print) ● ISSN 1785 0037 (Online)
DOI: http://dx.doi.org/10.15666/aeer/2104_32233241

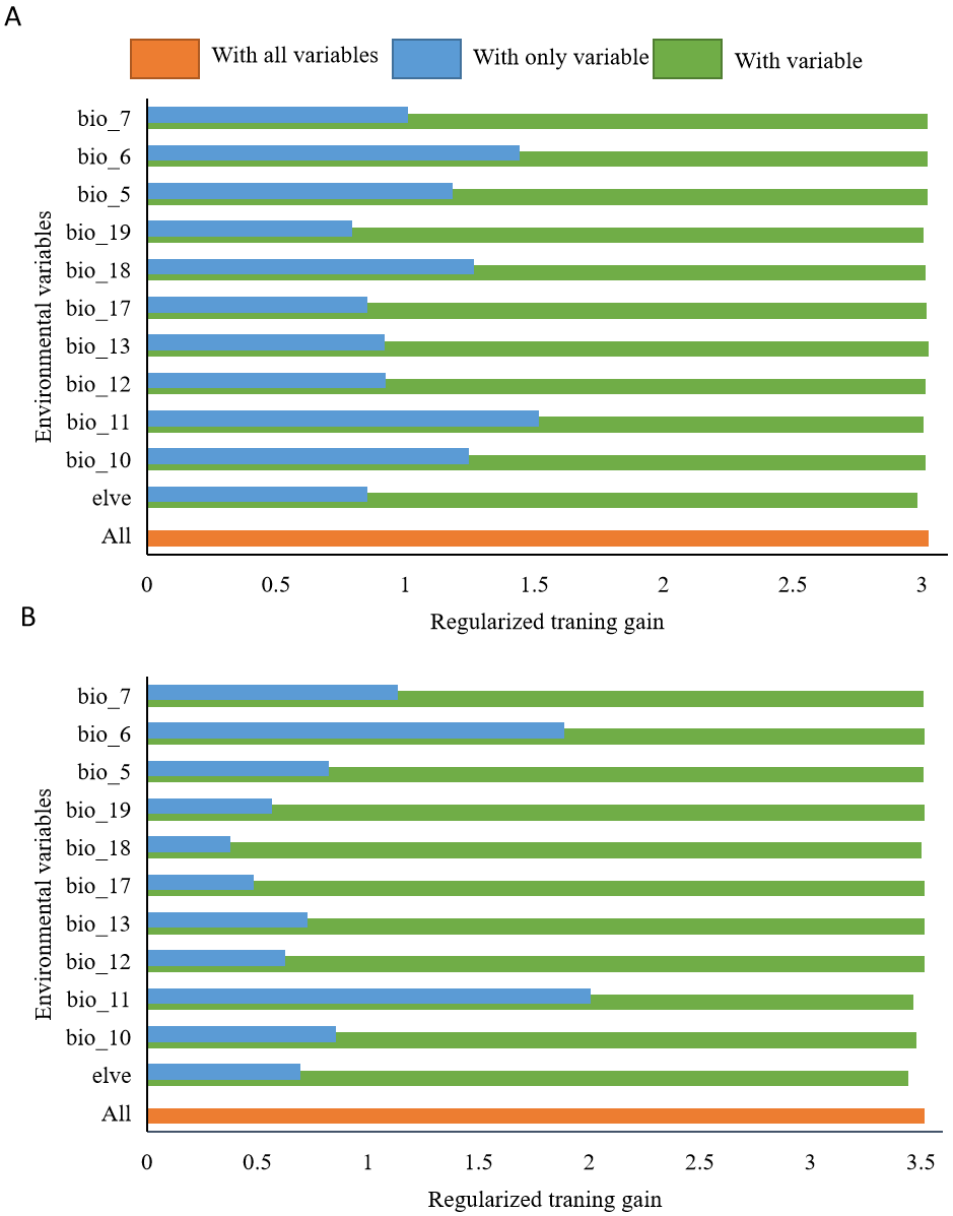

Figure 4. *Jackknife test results for Populus euphratica (A) and Populus pruinosa (B) bioclimatic variables*

Division of ecologically suitable areas of Pe and Pp under current climatic conditions and comparison of geographical distribution and niche

Under the current climate, *Pe* and *Pp* were mainly distributed in in northwest China, including Xinjiang, Gansu, Inner Mongolia (*Fig. 7*). According to the statistical results, the total area of *Pe* and *Pp* in China was 141.16×10^4 km^2 and 172.25×10^4 km^2, accounting for 14.65% and 16.88% of the total area of China mainland, respectively. The high-suitability area of *Pe* was 76.81×10^4 km^2, and the poorly-suitability area was 64.35×10^4 km^2. The high-suitability area of *Pp* was 60.38×10^4 km^2, and the poorly-suitability area was 111.86 km^2.

The niche overlap values of *Pe* and *Pp* were 0.533 and 0.775 respectively, with high niche overlap. The geographic distribution coincidence of *Pe* and *Pp* was 0.6119.

http://www.aloki.hu ● ISSN 1589 1623 (Print) ● ISSN 1785 0037 (Online)
DOI: http://dx.doi.org/10.15666/aeer/2104_32233241

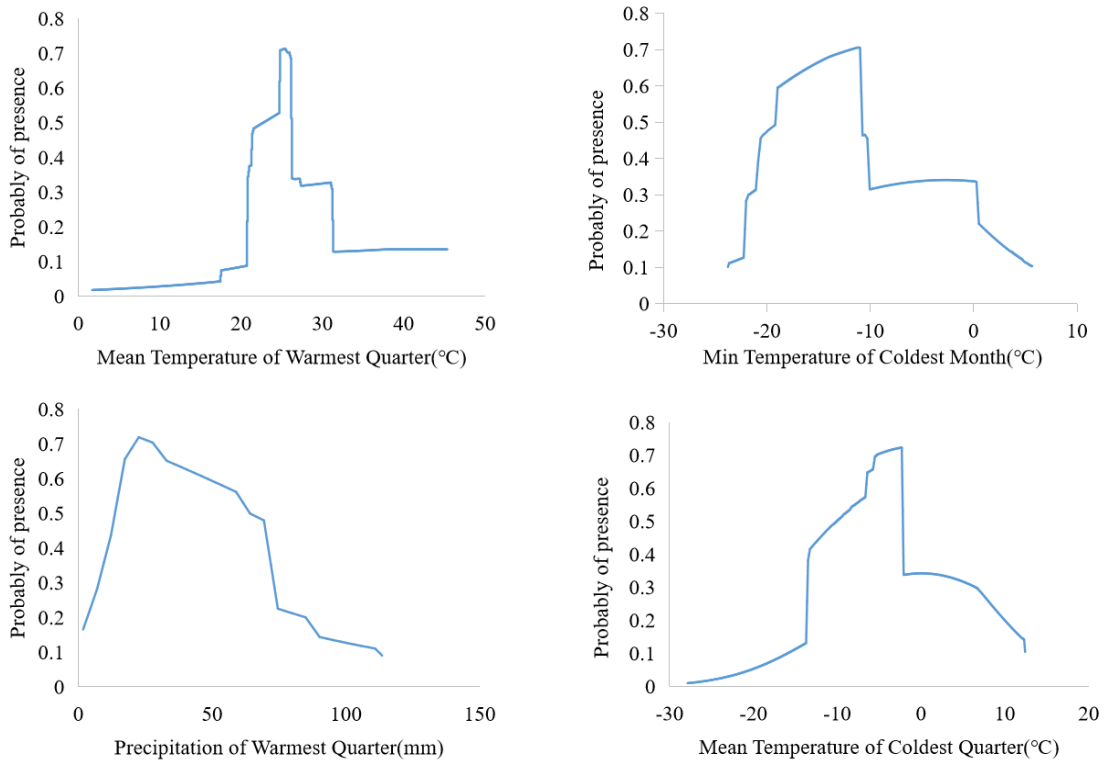

Figure 5. *Single response curve of dominant environmental factors of Populus euphratica*

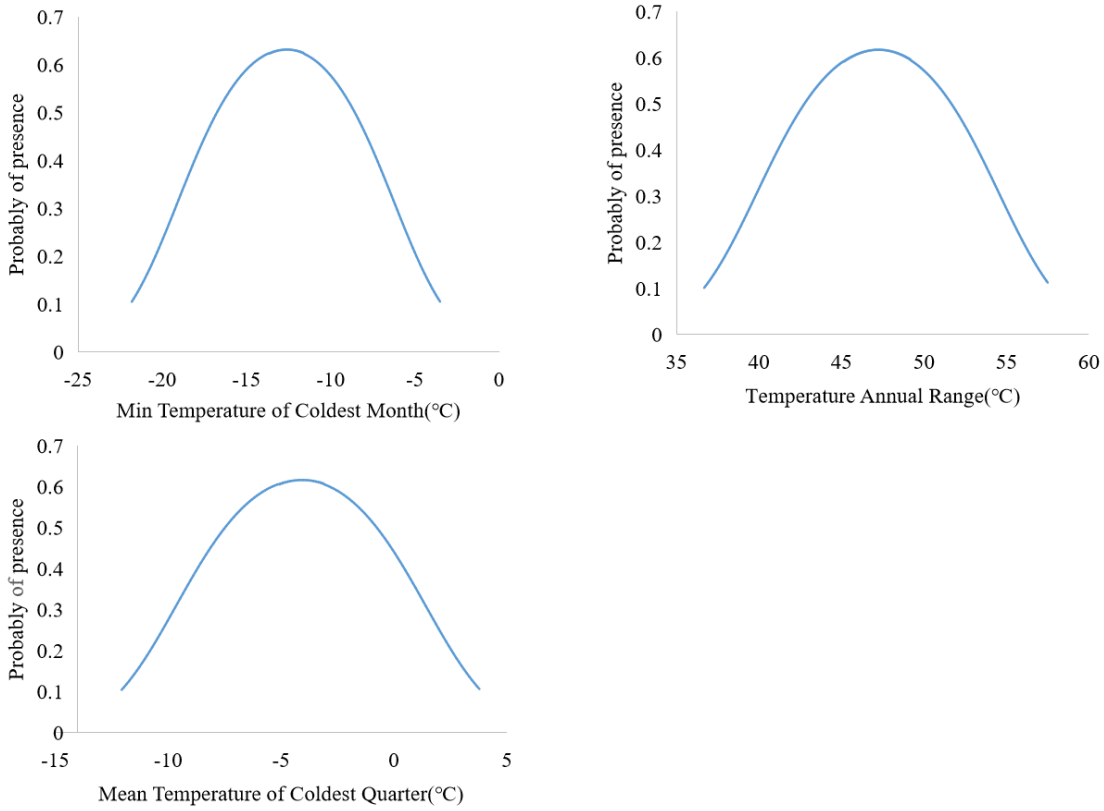

Figure 6. *Single response curve of dominant environmental factors of Populus pruinosa*

http://www.aloki.hu ● ISSN 1589 1623 (Print) ● ISSN 1785 0037 (Online)
DOI: http://dx.doi.org/10.15666/aeer/2104_32233241

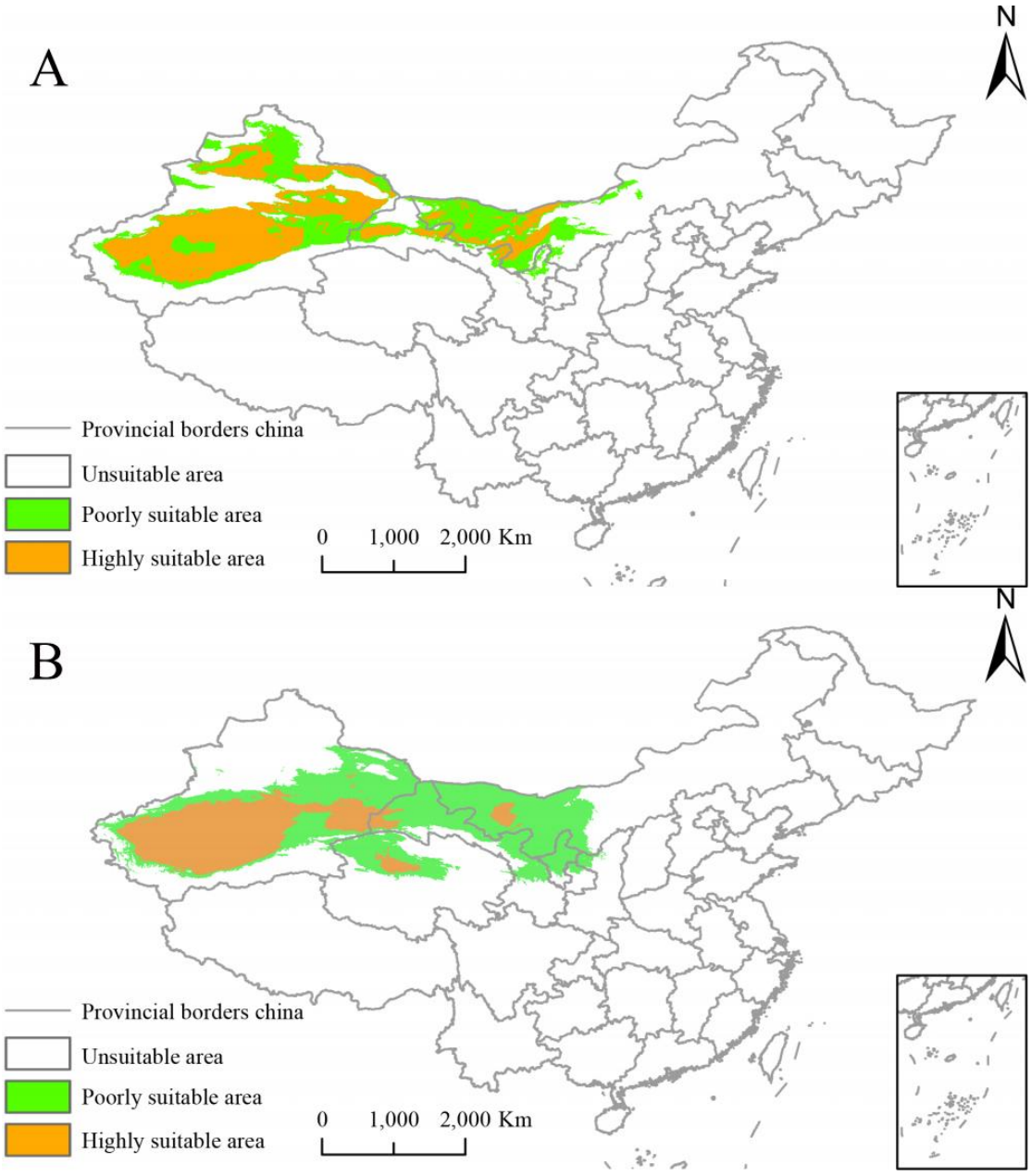

Figure 7. *The current potential suitable areas of Populus euphratica (A) and Populus pruinosa (B)*

Changes in the global distribution of Pe and Pp suitable areas under future climate conditions

In the 2050s, the total suitable area of *Pe* under the SSP1-2.6 scenario was 204.16×10^4 km^2, the poorly-fitness area was 110.83×10^4 km^2, and high-fitness area was 93.33×10^4 km^2. The total suitable area of *Pp* was 196.01×10^4 km^2, the poorly-fitness area was 80.52×10^4 km^2, and high-fitness area was 115.49×10^4 km^2. Under the SSP5-5.8 scenario in 2050s, the total suitable area of *Pe* was 208.16×10^4 km^2. the poorly-fitness area was 122.3×10^4 km^2, and high-fitness area was 85.85×10^4 km^2. The total suitable area of *Pp* was 188.83×10^4 km^2, the poorly-fitness area was

http://www.aloki.hu ● ISSN 1589 1623 (Print) ● ISSN 1785 0037 (Online)
DOI: http://dx.doi.org/10.15666/aeer/2104_32233241

80.79 × 10^4 km^2, and high-fitness area was 108.04 × 10^4 km^2. In the 2050s, under SSP1-2.6 and SSP5-5.8, the total suitable area, the poorly-fitness area, the high-fitness area of *Pe* and *Pp* were increased, except for the reduction of the poorly- fitness area of *Pp* (*Fig. 8; Table A1*).

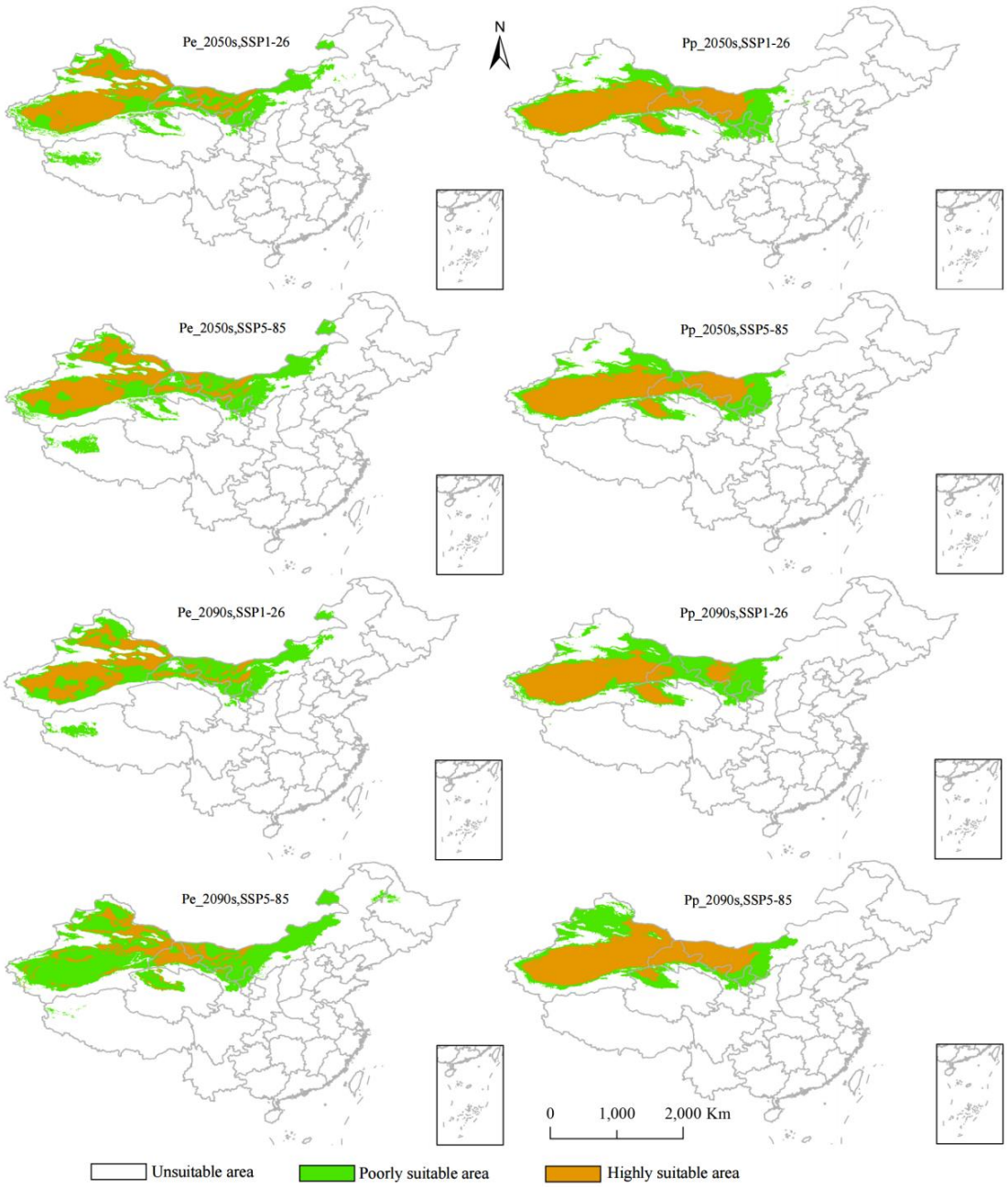

Figure 8. *Potential suitable areas of Populus euphratica and Populus pruinosa*

In the 2050s, the high-fitness areas of *Pe* lost under the SSP1-2.6 and SSP5-5.8 scenario were 4.05 × 10^4 km^2, 8.12 × 10^4 km^2, the increase in high-fitness areas were 18.89 × 10^4 km^2, 15.86 × 10^4 km^2. The high-fitness areas of *Pp* lost were 4.05 × 10^4 km^2, 2.07 × 10^4 km^2, the increase in high-fitness areas were 18.89 × 10^4 km^2, 46.56 × 10^4 km^2 (*Fig. 9; Table A1*).

http://www.aloki.hu ● ISSN 1589 1623 (Print) ● ISSN 1785 0037 (Online)
DOI: http://dx.doi.org/10.15666/aeer/2104_32233241

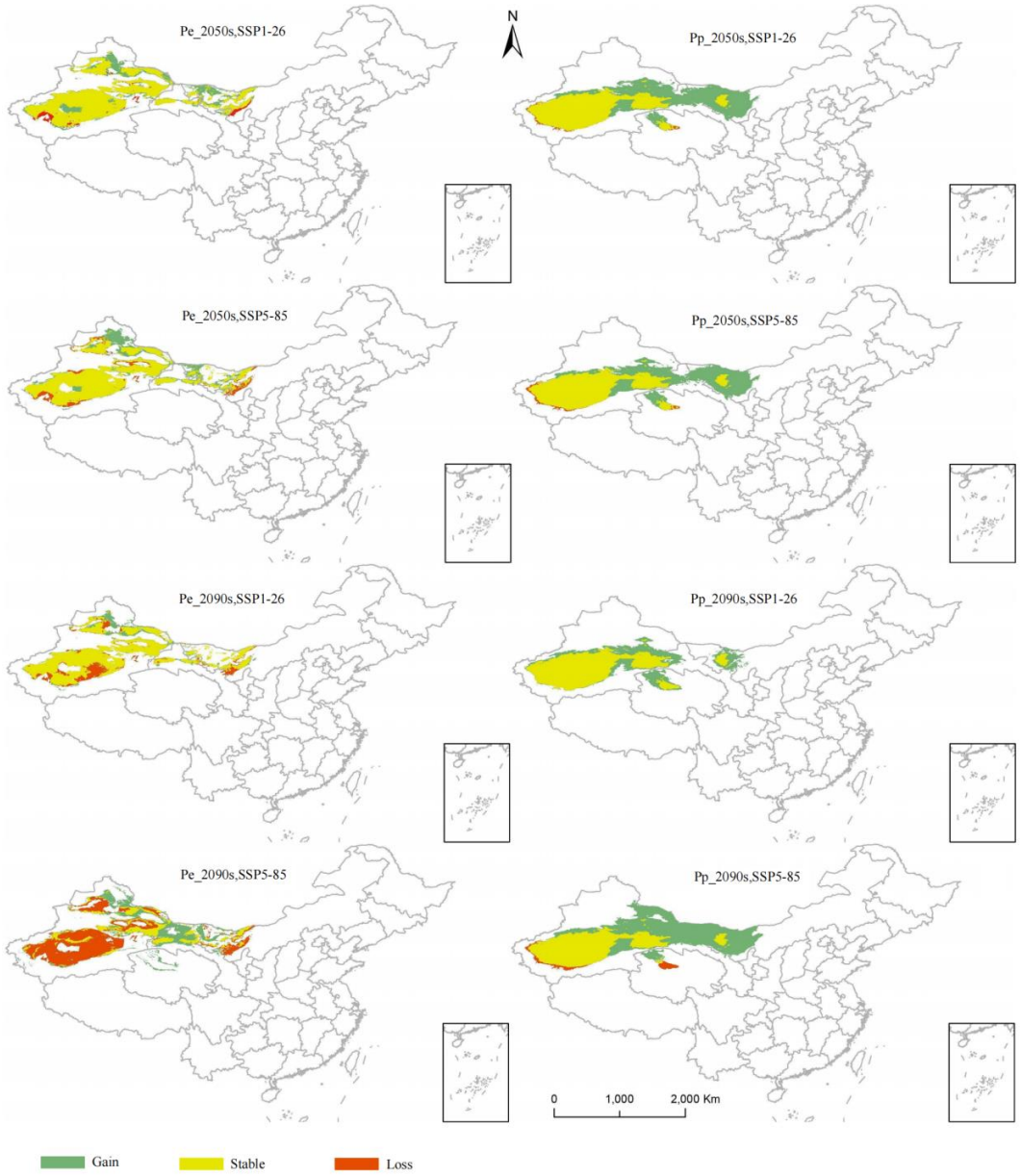

Figure 9. *The gain and loss of the suitable areas of Populus euphratica and Populus pruinosa in the future*

In the 2090s, the total suitable area of *Pe* under the SSP1-2.6 scenario was 189.91×10^4 km^2, the poorly-fitness area was 116.99×10^4 km^2, and high-fitness area was 92.92×10^4 km^2. The total suitable area of *Pp* was 188.65×10^4 km^2, the poorly-fitness area was 96.26×10^4 km^2, and high-fitness area was 92.39×10^4 km^2. Under the SSP5-5.8 scenario in 2090s, the total suitable area of *Pe* was 222.24×10^4 km^2. the poorly-fitness area was 171.29×10^4 km^2, and high-fitness area was 50.94×10^4 km^2. The total suitable area of *Pp* was 211.55×10^4 km^2, the poorly-fitness area was 82.87×10^4 km^2, and high-fitness area was 128.68×10^4 km^2. In the 2090s, under SSP1-2.6 and SSP5-5.8, the total suitable area and the poorly-fitness area of *Pe* were increased, the high-fitness area was decreased. The total suitable area and the high-fitness area of *Pp* were increased, the poorly-fitness area was decreased. (*Fig. 8; Table A1*).

http://www.aloki.hu ● ISSN 1589 1623 (Print) ● ISSN 1785 0037 (Online)
DOI: http://dx.doi.org/10.15666/aeer/2104_32233241

In the 2090s, the high-fitness areas of *Pe* lost under the SSP1-2.6 and SSP5-5.8 scenario were 11.97×10^4 km^2, 49.55×10^4 km^2. the increase in high-fitness areas were 7.89×10^4 km^2, 24.59×10^4 km^2. The high-fitness areas of *Pp* lost were 0 km^2, 4.63×10^4 km^2, the increase in high-fitness areas were 30.03×10^4 km^2, 67.46×10^4 km^2 (*Fig. 9; Table A1*).

The transfer of the center of Pe and Pp highly suitable areas under future climate conditions

The central coordinates of the *Pe* high-fitness area were 88.10°E, 40.83°N, located in Yuli County, Bayingolin Mongolian Autonomous Prefecture, Xinjiang Uygur Autonomous Region, China (*Fig. 10*). In the 2050s, under the SSP1-2.6 scenario, the central coordinates of the high-fitness area were 88.88°E, 41.19°N, under the SSP5-8.5 scenario, the central coordinates of the high-fitness area were 86.58°E, 41.34°N, and the moving distance were 69.66 km from the current to SSP1-2.6, 27.64 km from the SSP1-2.6 to SSP5-8.5. In the 2090s, under the SSP1-2.6 scenario, the central coordinates of the high-fitness area were 88.29°E, 41.30°N, under the SSP5-8.5 scenario, the central coordinates of the high-fitness area were 92.82°E, 41.90°N, and the moving distance were 54.13 km from the current to SSP1-2.6, 334.42 km from the SSP1-2.6 to SSP5-8.5.

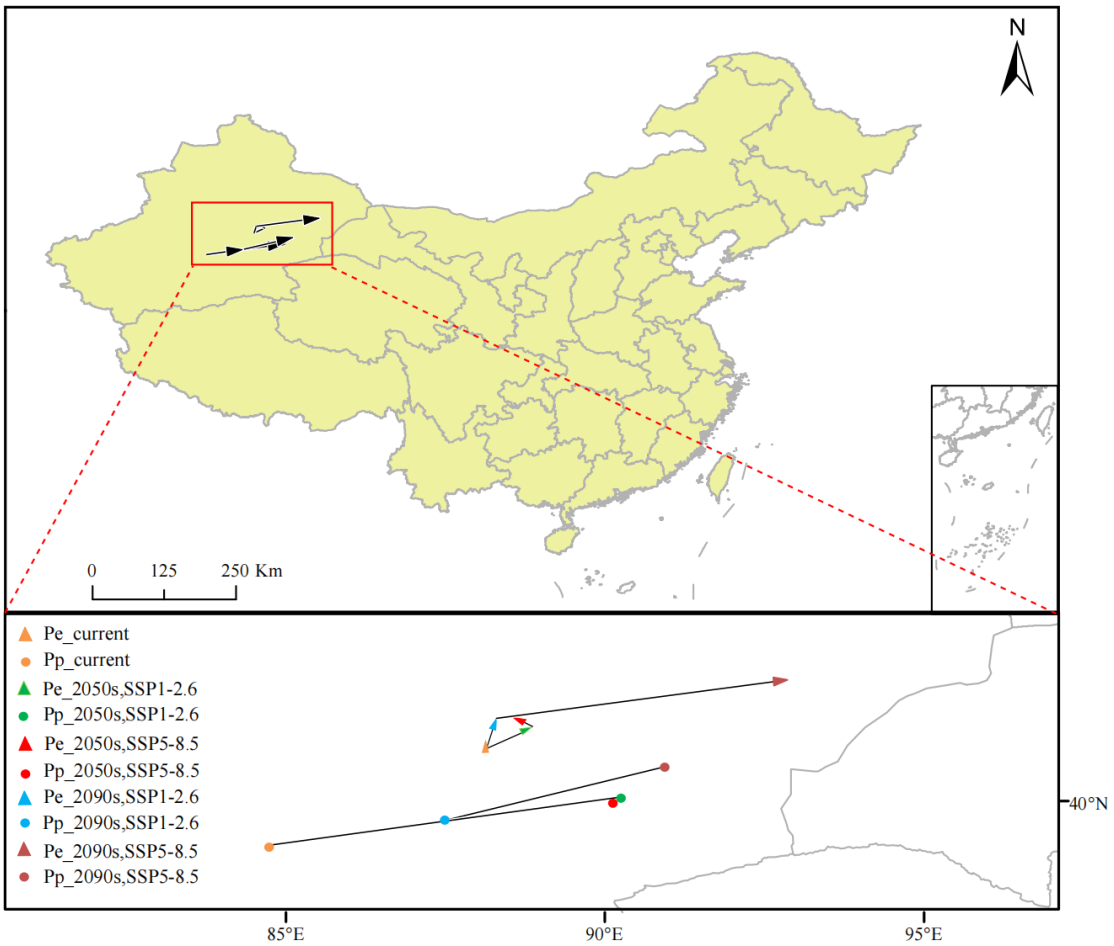

Figure 10. *The transfer of the center of the high-suitable area of Populus euphratica and Populus pruinosa*

http://www.aloki.hu ● ISSN 1589 1623 (Print) ● ISSN 1785 0037 (Online)
DOI: http://dx.doi.org/10.15666/aeer/2104_32233241

Under the current climate model, the central coordinates of the high-fitness area of *Pp* were 84.75°E and 39.31°N, located in Awati County, Aksu Prefecture, Xinjiang Uygur Autonomous Region, China (*Fig. 10*). In the 2050s, under the SSP1-2.6 scenario, the central coordinates of the high-fitness area were 90.31°E, 40.07°N, under the SSP5-8.5 scenario, the central coordinates of the high-fitness area were 90.07°E, 39.97°N, and the moving distance were 404.12 km from the current to SSP1-2.6, 20.47 km from the SSP1-2.6 to SSP5-8.5. In the 2090s, under the SSP1-2.6 scenario, the central coordinates of the high-fitness area were 87.41°E, 39.68°N, under the SSP5-8.5 scenario, the central coordinates of the high-fitness area were 90.93°E, 40.53°N, and the moving distance were 192.77 km from the current to SSP1-2.6, 269.54 km from the SSP1-2.6 to SSP5-8.5.

Discussion

Dominant environmental factors affecting the distribution of Pe and Pp

Under the current climate models, the distribution of *Pe* was affected by the coldest month minimum temperature (Bio6), the mean temperature of warmest quarter (Bio10), the coldest quarterly average temperature (Bio11) and the warmest quarterly precipitation (Bio18). The thresholds were -19 ~ -10℃, 22 ~ 26℃, -10 ~ -2℃ and 14 ~ 64 mm, respectively. The distribution of *Pp* was affected by the coldest month (Bio6), the temperature Annual Range (Bio7), and the average temperature in the coldest quarter (Bio11). The thresholds were -16 ~ -8℃, 42 ~ 52℃ and -7 ~ -1℃, respectively. The warmest quarterly precipitation (Bio18) was the key factor affecting the potential geographical distribution of *Pe* (Zhang et al., 2020). Li et al. (2020) found that the dominant variables affecting the distribution of *Pe* were the precipitation in the wettest month and the annual average temperature (Li et al., 2020). The distribution of *Pe* was limited by precipitation and temperature. This might be due to the fact that *Pe* growing on desert and dry river bed was greatly affected by the reduction of precipitation, which would affect the photosynthesis, growth and development of plants, as well as the maturity of seeds, thus limiting the expansion of *Pe* population. In addition, high temperature and low temperature stress would directly affect the enzyme activity in plants, thus affecting the life activities of plants. The distribution of *Pp* was limited by temperature, which might be due to the formation of forests on the floodplain where the *Pp* river overflows, and the high water content in the soil, which was less limited by precipitation. In addition, compared with *Pe*, *Pp* was not resistant to low temperature, which might be one of the reasons why the latitude range of pp distribution was smaller than that of *Pe*.

Distribution area of Pe and Pp

The suitable area of *Pe* was mainly distributed in Xinjiang, northwestern Gansu, western Inner Mongolia, while the suitable area of *Pp* was mainly distributed in southern Xinjiang. The simulated suitable area of *Pe* and *Pp* in this study was larger than the actual distribution area. Same as other research results (Zhuang et al., 2018). The possible reason was that the distribution of species was not only affected by climate and elevation variables, but also by soil, hydrological data, and other variables, followed by the migration ability of species and their reproductive ability, resulting in species unable to reach a suitable growth environment (Soberon et al., 2005). Both *Pe*

http://www.aloki.hu ● ISSN 1589 1623 (Print) ● ISSN 1785 0037 (Online)
DOI: http://dx.doi.org/10.15666/aeer/2104_32233241

and *Pp* could reproduce through seeds and clones, but in these two cases, the migration ability and reproduction ability of *Pe* and *Pp* were very limited. Seed germination requires soft silt and sufficient water. Clonal reproduction relied on developed roots, which limited the distance of reproduction.

At present, the predicted suitable area of *Pe* and *Pp* were larger than the actual area because the distribution of species was affected not only by climate, terrain, soil, and other environmental variables but also by many factors that were not considered. For example, it was restricted by the migration ability of species, farmland reclamation, urban planning, and other human disturbances. Second, although MaxEnt was superior to other modelling methods in achieving high prediction performance using only existing data. However, similar to other niche prediction models, there were inevitable limitations. Although data collection had been conducted from various aspects, there might be an incomplete collection of geographic information data of *Pe* and *Pp*.

Under the scenarios of the 2050s, SSP1-2.6 and SSP5-5.8, the high-fitness area of *Pe* increased 14.84×10^4 km^2, 7.744×10^4 km^2, respectively. Under the scenarios of the 2090s, SSP1-2.6 and SSP5-5.8, the high-fitness area of *Pe* decreased 4.08×10^4 km^2, 24.96×10^4 km^2, respectively. The results showed that future climate change was unfavorable to the survival of *Pe*. Zhang et al. (2020) showed that the area of potentially suitable areas for different grades of *Pe* had been reduced to different degrees compared with the current potentially suitable area (Zhang et al., 2020), which was consistent with the current research results. The current distribution of *P. euphratica* in this study was located between Zhang et al. (2020) and Li et al. (2020), which might be due to differences in model operation mode and climate factors (Zhang et al., 2020; Li et al., 2020) (*Table A1*). In the future, the temperature would rise, and the higher temperature would lead to a decrease in precipitation and drought (Liu et al., 2021). The closer to the inland area a site was, the less precipitation there was, so the range of the *Pe* high-fitness area in Central Asia was reduced.

With climate change in the future, under the scenarios of the 2050s, SSP1-2.6, SSP5-5.8, and 2090s, SSP2-2.6, SSP5-5.8, the high-fitness area of *Pp* increased 14.84×10^4 km^2, 43.49×10^4 km^2, 30.03×10^4 km^2 and 62.83×10^4 km^2, respectively. The results showed that future climate change was more favorable to the survival of *Pp*. Under the scenarios of the 2090s, SSP5-5.8, *Pp* had the largest high-fitness area. This might be because the temperature increases under this condition, which was just within the appropriate range of *Pp*, and further explains the weak low temperature resistance of *Pp*.

The niche overlap and geographic distribution coincidence of Pe and Pp

According to the simulation results of *Pe* and *Pp* under the current climate, the niche overlap D and I values of *Pe* and *Pp* were 0.533 and 0.775 respectively, with high niche overlap. The geographic distribution coincidence of *Pe* and *Pp* was 0.6119. The selection and response of the two species to environmental factors showed some differences, which might be one of the reasons why the two species could adapt to each other and coexist stably for a long time in the case of large areas of overlapping habitats.

The change in the high-fitness area center of Pe and Pp under future climate

The results showed that the centroid of potentially suitable area of *Pe* and *Pp* in China shifted to high-latitude areas under future climate scenarios. This result is

http://www.aloki.hu ● ISSN 1589 1623 (Print) ● ISSN 1785 0037 (Online)
DOI: http://dx.doi.org/10.15666/aeer/2104_32233241

consistent with the moving direction of the center of the future adaptive zone of most plants (Bandh et al., 2021; Hou et al., 2021; Yu et al., 2019; Mao et al., 2017). Zhang's research results showed that the potentially suitable area of *Pe* will migrate to the high-altitude area as a whole (Zhang et al., 2020).

Conservation strategies of Pe and Pp resources

Based on the current and future prediction results of *Pe* and *Pp*, *Pe* was selected as a protected species. However, compared with *Pe*, *Pp* has a narrower distribution area, and its low temperature and drought resistance is poor. Therefore, the conservation of *Pe* and *Pp* should not only consider the reduction in population in future suitable areas but also ensure that good protection measures are provided for the stability of the population. It is also necessary to consider the current population with a narrow distribution of suitable living areas, which is conducive to the expansion of narrow suitable living areas. Moreover, combining the existing genetic diversity results of *Pe* and *Pp* in our laboratory, both had low genetic diversity in northern Xinjiang, China, and high genetic diversity in southern Xinjiang (Chen et al., 2021b; Warren et al., 2021). However, the populations of *Pe* and *Pp* in southern Xinjiang had more abundant genetic diversity and ancient resources of *Pe* and *Pp* than those in northern Xinjiang, and the drought degree in southern Xinjiang was more serious than that in northern Xinjiang. Therefore, the protection of the diversity of *Pe* and *Pp* should not only consider populations with rich genetic diversity but also ensure a rich gene pool for the expansion of the population. It is also necessary to consider the low genetic diversity population preserved by natural selection, which is helpful to excavate excellent genotypes suitable for the specific natural ecological environment. Therefore, the protection of *Pe* and *Pp* resources in the future should focus on the whole Xinjiang region of China.

In addition, ecological water conveyance projects could be implemented in key protected areas, and scientific ecological water conveyance measures could be taken according to the physical conditions of key protected areas (Fan et al., 2013). Through the establishment of natural reserves, gene resource protection bases, germplasm resource banks and other forms, the in-place protection and off-site protection of pe and pp high-quality resources would be realized (Gai et al., 2021).

Conclusions

Based on the optimized MaxEnt model and environmental variables to predict suitable habitats of *Pe* and *Pp*. The study concluded that (1) the significant environmental variables influencing the Distribution area of *Pe* were the coldest month minimum temperature (Bio6), the mean Temperature of Warmest Quarter (Bio10), the coldest quarterly average temperature (Bio11) and the warmest quarterly precipitation (Bio18); the significant environmental variables influencing the Distribution area of *Pp* were The coldest month minimum temperature (Bio6), the temperature Annual Range (Bio7), and the coldest quarterly average temperature (Bio11). (2) The suitable area of *Pe* was mainly distributed in Xinjiang, northwestern Gansu, western Inner Mongolia, while the suitable area of *Pp* was mainly distributed in southern Xinjiang. (3) *Pe* and *Pp* have high niche overlap and geographic distribution coincidence. (4) Under the future climate scenario, the potential high-fitness area of *Pe* and *Pp* would shift to higher latitudes.

http://www.aloki.hu ● ISSN 1589 1623 (Print) ● ISSN 1785 0037 (Online)
DOI: http://dx.doi.org/10.15666/aeer/2104_32233241

Funding. This work was supported by Bingtuan Science and Technology Program (Funding number: 2022CB001-10; 2021BB010) and The Third Scientific Research Project in Xinjiang (Funding number: 2022xjkk0200/2022xjkk0204). This work was also supported by President's Fund Project of Tarim University (Funding number: TDZKKY202202). This work was also supported by the Graduate Research Innovation Project of the Xinjiang Uygur Autonomous Region（Funding number: XJ2020G268).

Competing interests. The authors declared that they had no conflict of interests.

Availability of data and materials. The datasets generated and/or analyzed during the current study are available on the website of the World Climate Database (WorldClim; https: //www.worldclim.org/), National Oceanic and Atmospheric Administration (NOAA-NCEI; https://www.ngdc.noaa. gov/) and Global Biodiversity Information network (https://www.gbif.org/).

REFERENCES

[1] Anand, V., Oinam, B., Singh, I. H. (2021): Predicting the current and future potential spatial distribution of endangered *Rucervus eldii eldii* (Sangai) using MaxEnt model. – Environmental Monitoring Assessment 193(3): 147.

[2] Bandh, S. A., Shafi, S., Peerzada, M. (2021): Multidimensional analysis of global climate change: a review. – Environmental Science Pollution Research International 28(20): 24872-24888.

[3] Brown, J. L., Bennett, J. R., French, C. M. (2017): SDMtoolbox 2.0: the next generation Python-based GIS toolkit for landscape genetic, biogeographic and species distribution model analyses. – PeerJ 5: e4095.

[4] Chen, H., Nie, Y., Liu, X., Liu, B., Zhang, H. (2021a): Research on prediction of potential suitable areas of *populus euphratica* based on MaxEnt model. – China Agriculture Information 33(1): 46-55.

[5] Chen, X. X., Gai, Z. S., Zhai, J. T. (2021b): Genetic diversity and construction of core conservation units of the natural populations of *Populus euphratica* in Northwest China. – Biodiversity Science 29(12): 1638-1649.

[6] Cobos, M. E., Peterson, A. T., Barve, N. (2019): kuenm: an R package for detailed development of ecological niche models using Maxent. – PeerJ 7: e6281.

[7] Cong, M., Xu, Y., Tang, L., Yang, W., Jian, M. (2020): Predicting the dynamic distribution of Sphagnum bogs in China under climate change since the last interglacial period. – PloS one 15(4): e0230969.

[8] Dai, X., Wu, W., Ji, L., Tian, S., Yang, B., Guan, B., Wu, D. (2022): Parnassia wightiana MaxEnt model-based prediction of potential distributions of (*Celastraceae*) in China. – Biodiversity data journal 10: e81073.

[9] Dan, L. W., Glor, R. E., Turelli, M. (2010): ENMTools: a toolbox for comparative studies of environmental niche models. – Ecography 33: 607-611.

[10] Elith, J., Phillips., S. J., Trevor, H., Dudik, M., Chee, Y. E., Yates, C. J. (2011): A statistical explanation of MaxEnt for ecologists. – Diversity Distributions 17(1): 43-57.

[11] Fan, Z. L., Hai-Liang, X. U., Jin-Yi, F. U. (2013): Ecological protection objects and restoration measures in the lower reaches of Tarim River. – Journal of Desert Research 33(4): 1191-1197.

[12] Fourcade, Y., Secondi, J., Valentine, J. F. (2014): Mapping species distributions with MAXENT using a geographically biased sample of presence data: a performance assessment of methods for correcting sampling bias. – Plos One 9(5): e97122.

[13] Fourcade, Y., Besnard, A. G., Secondi, J. (2018): Paintings predict the distribution of species! or the challenge of selecting environmental predictors and evaluation statistics. – Global Ecology & Biogeography 27(2): 245-256.

[14] Gai, Z., Zhai, J., Chen, X. (2021): *Populus* Phylogeography Reveals Geographic and Environmental Factors Driving Genetic Differentiation of sect. Turanga in Northwest China. – Frontiers in Plant Science 12: 705083.

http://www.aloki.hu ● ISSN 1589 1623 (Print) ● ISSN 1785 0037 (Online)
DOI: http://dx.doi.org/10.15666/aeer/2104_32233241

[15] Gomes, V., Ijff, S. D., Raes, N. (2018): Species distribution modelling: contrasting presence-only models with plot abundance data. – Scientific Reports 8(1): 1003.
[16] Guan, L., Yang, Y., Jiang, P., Mou, Q., Wang, R. (2022): Potential distribution of *Blumea balsamifera* in China using MaxEnt and the ex situ conservation based on its effective components and fresh leaf yield. – Environmental Science and Pollution Research International 29: 44003-44019.
[17] Guisan, A., Thuiller, W. (2004): Predicting species distribution: offering more than simple habitat models. – Ecology Letters 10(5): 435-435.
[18] Guisan, A., Zimmermann, N. E. (2000): Predictive habitat distribution models in ecology. – Ecological Modelling 135(2-3): 147-186.
[19] Guo, Y., Li, X., Zhao, Z. (2017): Prediction of the potential geographic distribution of the ectomycorrhizal mushroom Tricholoma matsutake under multiple climate change scenarios. – Scientific Reports 7: 46221.
[20] Hanley, J. (1982): The meaning and use of the area under a receiver operating characteristic (ROC) curve. – Radiology 143(1): 29-36.
[21] Hebbar, K. B., Abhin, P. S., Sanjo Jose, V., Neethu, P., Santhosh, A., Shil, S., Prasad, P. V. V. (2022): Cocos nucifera predicting the potential suitable climate for coconut (*Cocos nucifera* L.) Cultivation in India under climate change scenarios using the MaxEnt Model. – Plants 11(6): 731.
[22] Hou, Y., Wang, Q. (2021): A bibliometric study about energy, environment, and climate change. – Environmental Science Pollution Research International 28(26): 34187-34199.
[23] Li, J., Guo, H., Wang, Y., Xin, Z., Li, Y. (2020): Identification of potential distribution area for *Populus euphratica* by the MaxEnt ecologic niche model. – Scientia Silvae Sinicae 55(12): 133-139.
[24] Li, M., Xian, X., Zhao, H. (2022a): Predicting the potential suitable area of the invasive ant *Linepithema humile* in China under future climatic scenarios based on optimized MaxEnt. – Diversity 14(11): 921.
[25] Li, Y., Shao, W., Jiang, J. (2022b): Predicting the potential global distribution of *Sapindus mukorossi* under climate change based on MaxEnt modelling. – Environmental Science Pollution Research International 29(15): 21751-21768.
[26] Liu, C. R., White, M., Newell, G. (2013): Selecting thresholds for the prediction of species occurrence with presence-only data. – Journal of Biogeography 40(4): 778-789.
[27] Liu, Y. R., Yang, X., Huang, G. H. (2021): Development of an integrated multivariate trend-frequency analysis method: spatial-temporal characteristics of climate extremes under global warming for Central Asia. – Environmental Research 195: 110859.
[28] Manzoor, S. A., Griffiths, G., Lukac, M. (2020): Land use and climate change interaction triggers contrasting trajectories of biological invasion. – Ecological Indicators 120: 1470-160X.
[29] Mao, L., Li, Y., Liu, C., Fang, Y. M. (2017): Predication of potential distribution of *Haplocladium microphyllum* in China based on MaxEnt model. – Chinese Journal of Ecology 36(1): 54-56.
[30] Moreno, R., Zamora, R., Molina, R. J., Vasquez, A., Herrera, M. A. (2011): Predictive modeling of microhabitats for endemic birds in South Chilean temperate forests using Maximum entropy (Maxent). – Ecological Informatics 6(6): 364-370.
[31] Pennino, M. G., Vilela, R., Bellido, J. M. (2018): Effects of environmental data temporal resolution on the performance of species distribution models. – Journal of Marine Systems 189: 78-86.
[32] Peterson, A. T. (2006): Uses and requirements of ecological niche models and related distributional models. – Biodiversity Informatics 3: 59-72.
[33] Phillips, S. J., Dudík, M., Elith, J. (2009): Sample selection bias and presence-only distribution models: implications for background and pseudo-absence data. – Ecological Applications 19(1): 181-197.

http://www.aloki.hu ● ISSN 1589 1623 (Print) ● ISSN 1785 0037 (Online)
DOI: http://dx.doi.org/10.15666/aeer/2104_32233241

[34] Soberon, J., A., Townsend, P. (2005): Interpretation of models of fundamental ecological niches and species' distributional areas. – Biodiversity Informatics 2: 1-10.
[35] Wang, S. J., Chen, B. H., Li, H. Q. (1995): Euphrates Poplar Forest. – Environmental Science Press, Beijing.
[36] Wang, J., Wu, Y., Ren, G. (2011): Genetic differentiation and delimitation between ecologically diverged *Populus euphratica* and *P. pruinosa*. – PloS One 6: e26530.
[37] Wang, J., Källman, T., Liu, J. (2014): Speciation of two desert poplar species triggered by Pleistocene climatic oscillations. – Heredity 112(2): 156-164.
[38] Wang, R. L., Li, Q., Feng, C. H., Shi, Z. P. (2017): Predicting potential ecological distribution of *Locusta migratoria tibetensis* in China using MaxEnt ecological niche modeling. – Acta Ecologica Sinica 37(24): 423-433.
[39] Wang, Y., Chao, B., Dong, P. (2021): Simulating spatial change of mangrove habitat under the impact of coastal land use: coupling MaxEnt and Dyna-CLUE models. – Science of The Total Environment 788: 147914.
[40] Warren, D. L., Matzke, N. J., Cardillo, M. (2021): ENMTools 1.0: An R package for comparative ecological biogeography. – Ecography 44(4): 504-511.
[41] Yan, W. B., Wang, Q., Chao, W. (2015): Evaluation of potential breeding habitat distribution with maxent model for crested ibis in the Qinling-Bashan Region. – Chinese Journal of Zoology 50(2): 185-193.
[42] Yi, Y. J.., Hong, S., Xi, C., Yang, Z. (2016): Maxent modeling for predicting the potential distribution of endangered medicinal plant (H. *riparia Lour*) in Yunnan, China. – Ecological Engineering 92: 260-269.
[43] Yu, F., Wang, T., Groen, T. A., et al. (2019): Climate and land use changes will degrade the distribution of *Rhododendrons* in China. – Science of The Total Environment 659(1): 515-528.
[44] Zeng, Y. F., Zhang, J. G., Abuduhamiti, B. (2018): Phylogeographic patterns of the desert poplar in Northwest China shaped by both geology and climatic oscillations. – BMC Evolutionary Biology 18(1): 75.
[45] Zhang, H., Zhao, H. X., Wang, H.（2020): Potential geographical distribution of *Populus euphratica* in China under future climate change scenarios based on Maxent model. – Acta Ecologica Sinica 40(18): 6552-6563.
[46] Zhou, R., Gao, Y., Chang, N. (2022): Potential distribution of *Triatoma rubrofasciata* under different climatic scenarios in China. – Chin J Vector Biol & Control 33: 125-132.
[47] Zhu, G., Liu, Q., Gao, Y. (2014): Improving ecological niche model transferability to predict the potential distribution of invasive exotic species. – Biodiversity Science 22(2): 223-230.
[48] Zhuang, H., Qin, H., Wang, W., Zhang, Y. (2018): Prediction of the potential suitable distribution of *Taxus Yunnanensis* Based on MaxEnt model. – Journal of Shanxi University 41(1): 233-240.

http://www.aloki.hu ● ISSN 1589 1623 (Print) ● ISSN 1785 0037 (Online)
DOI: http://dx.doi.org/10.15666/aeer/2104_32233241

APPENDIX

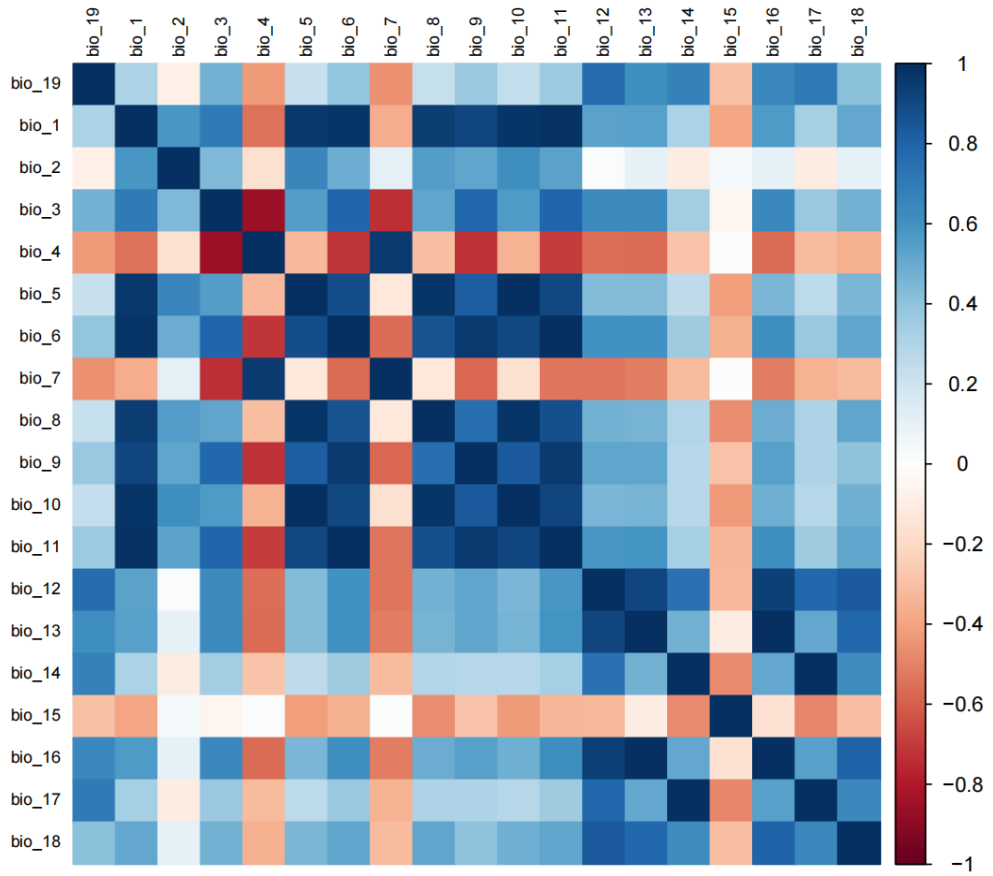

Figure A1. *Correlation analysis of 19 climatic data*

Table A1. *Suitable areas for Pe under different climate change scenarios in different articles*

Period	Current ($\times 10^4$ km^2)	2050s, 126/256 ($\times 10^4$ km^2)	2070, 126/245/360/585 ($\times 10^4$ km^2)	2090s, 126/256 ($\times 10^4$ km^2)	Actual ($\times 10^4$ km^2)
Li et al. (2020)	112.03	-	-	-	0.65
Zhang et al. (2020)	289.94	-	121.81/125.28/125.82/125.93	-	0.65
Chen et al. (2021)	1.01	-	-	-	0.65
This study	141.16	204.16/208.16	-	189.91/222.24	0.65

Chen et al. (2021) just include Aksu River basin, Xin Jang. The actual distribution areas of *Pe* came from Wang et al. (1995)

Table A2. *Suitable areas for Pe and Pp under different climate change scenarios*

Period	Current ($\times 10^4$ km^2)	2050s, 126 ($\times 10^4$ km^2)	2050s, 585 ($\times 10^4$ km^2)	2090s, 126 ($\times 10^4$ km^2)	2090s, 585 ($\times 10^4$ km^2)	Actual ($\times 10^4$ km^2)
Total area of *Pe*	141.16	204.16	208.16	189.91	222.24	0.65
Total area of *Pp*	172.25	196.01	188.83	188.65	211.55	0.30
High-suitability area of *Pe*	76.81	93.33	85.85	92.92	50.94	-
High-suitability area of *Pp*	60.38	115.49	108.04	92.39	128.68	-
poor-suitability area of *Pe*	64.35	110.83	122.3	116.99	171.29	-
poor-suitability area of *Pp*	111.86	80.52	80.79	96.26	82.87	-

The actual distribution areas of *Pe* and *Pp* came from Wang et al. (1995)

http://www.aloki.hu ● ISSN 1589 1623 (Print) ● ISSN 1785 0037 (Online)
DOI: http://dx.doi.org/10.15666/aeer/2104_32233241